Electrochimica Acta 128 (2014) 102–112

Contents lists available at ScienceDirect

Electrochimica Acta

journal homepage: www.elsevier.com/locate/electacta

Do Carbon Nanotubes contribute to Electrochemical Biosensing?

Sandro Carrara*, Camilla Baj-Rossi, Cristina Boero, Giovanni De Micheli

EPFL - École Polytechnique Fédérale de Lausanne (CH)

ARTICLE INFO

Article history:
Received 7 July 2013
Received in revised form
18 December 2013
Accepted 19 December 2013
Available online 4 January 2014

Keywords:
Carbon Nanotubes
Electrochemical Sensors
Nernst
Cottrell
Randle-Sevčick

ABSTRACT

Carbon nanotubes have been attracting a lot of interest as electron transfer mediators to enhance electrochemical biosensing. The main reason behind this is usually recognized in terms of augmented electrochemical active surface area. The aim of this paper is to review other phenomena that occur at the electrochemical interface. Three distinct features of these phenomena mainly appear in electrochemical biosensing. We introduce the Cottrell, Randle-Sevčick, and Nernst effects to address these features. By using these features, several electrochemical biosensing systems are investigated. Differences among the proposed systems are presented and analyzed in light of these effects. We finally have demonstrated that carbon nanotubes may induce completely opposite effects when dealing with different biosensing systems. This paper also shows that even seemingly small differences (*e.g.*, changing metabolite as detected by the same enzyme) might result in opposite effects on the same carbon nanotube based sensor. Nevertheless, it is shown that carbon nanotubes, in some cases, confirm their exceptional nature in enhancing the sensor performance by orders of magnitude. The sensitivity increases from 87 ± 62 to 3718 ± 73 nA/μM $\times$cm^2 and detection limit decreases from 7.5 ± 5.3 mM to 84 ± 2 μM in case of cyclophosphamide detected by the cytochromes P450 3A4.

1. Introduction

It has been recognized in 1997 [1] and confirmed in 2006 [2] that *Carbon Nanotubes* (CNT) have been pointed out to the general scientific community only in 1991 [3]. They have been actually discovered only in 1993 in the form of *Single Walled* (SWCNT) [4,5]. However, their first observation was much earlier. The true discovery of carbon filaments in the form of tubes with diameter in the nanometer-scale dates back to 1952 [6] and in 1958 the first evidence of concentric textures was published [7], as we usually find in the form of *Multi-Walled* (MWCNT). Several works published in the 70s have then contributed to the characterization of these new nano-sized structures [8]. After the paper published in 1991, they have been proposed for a huge plethora of different applications: substrates for drug delivery [9,10], nano-tips for electrons field-emission [11], composites to improve mechanical properties of materials [12–14], hydrogen-storage building-blocks for fuel-cells [15], quantum wires [16], ballistic conductors [17], molecular transistors [18] and sensors for gas ionization [19], liquid flow [20], near-infrared light [21], pressure [22], or molecular-recognition [23].

In the field of biosensing, carbon nanotubes have also been proposed for electrochemical detection. Several sensors have been suggested based on carbon nanotubes and enzyme-mediators such as glucose oxidase [24], l-Amino acid oxidase [25], cholesterol oxidase/esterase [26], acetylcholinesterase [27], lactate oxidase [28] cytochrome C [29], cytochrome P450 [30], glucose oxidase/hexokinase [31]. The direct electron transfer between carbon nanotubes and electrochemically active molecules has been demonstrated as well. Small molecules such as hydrogen peroxide [32], potassium ferricyanide [33], dopamine [34], and etoposide [35] have been detected with electrochemical techniques.

The main conclusion we can deduce from this vast literature is that carbon nanotubes have an impact in terms of sensitivity and limit of detection. The simplest explanation is that the inherent high surface area of carbon nanotubes contributes to the electrochemically active area of the working electrode (WE). While this argument is undoubtedly true, it is not enough to explain their role in electrochemical biosensing. Initially, some peculiar explanations were proposed. For example, it has been suggested that SWCNTs "are able to 'pierce' the glycoprotein shell of the GOx [Glucose Oxidase] and gain access to the redox sites and be established within tunneling distance of the redox active co-factor (FAD) of the enzyme" [24], or that MWCNTs are contributing because "similarity in length scales between nanotubes and redox enzymes suggests interactions that may be favorable" [26]. Later on, deep investigations have pointed out the phenomena involved. Carbon was being lined up in the tubes in such a way that it provided high electrochemical activity [25] while functionalized sidewalls were inducing more enzyme adsorption [28]. Carbon nanotubes "have fast

* Corresponding author.
E-mail address: Sandro.carrara@epfl.ch (S. Carrara).

0013-4686/$ – see front matter © 2014 Elsevier Ltd. All rights reserved.
http://dx.doi.org/10.1016/j.electacta.2013.12.123

electron transfer rates similar to a graphite edge-plane electrode, while the side-walls present very slow electron transfer rates similar to the graphitic basal plane"[27]. It has been demonstrated that the edge-plane sites and tube ends are the reactive sites for an efficient heterogeneous electron-transfer at the electrode/electrolyte interface [36,37]. In a similar manner, plane defects [38] and presence of impurities [39] along the sidewall surface also increase the heterogeneous electron-transfer. This is a key finding that is very clear now. However, several details of the electron-transfer process to/from the tubes are still unclear and the topic is still debated today [40] because "questions remain regarding the fundamental electrochemical properties of CNTs, that need to be resolved for the field to advance in a rational manner"[41].

For example, it was found that the usual semi-infinite planar diffusion model is not accurate enough to fully explain cyclic voltammetry because thin layer effects likely operate even in simple cases such as the oxidation of ferrocyanide on glassy carbon electrodes modified with SWCNT [42]. However, we will see that thin layer effects explain peak shifts occurring on hydrogen peroxide while do not support peaks shift on etoposide and ferrocyanide on MWCNT. Moreover, "heterogeneous electrochemical processes are further complicated by the fact that the vast majority of electrode/electrolyte systems involve solid electrodes that have spatially non uniform properties which may impact significantly on the local activity" [40] while more complex electrochemical systems are usually involved in biosensing with the integration of very large biomolecules such as enzymes that provide direct electron transfer.

Although it is very easy to agree that CNT "can promote electron transfer and enhance the response current" [26], the mechanism of electron transfer between CNT and large biomolecules is, however, still not fully understood, especially considering the differences found between very similar systems [43].

Therefore, the aim of this paper is to propose an original way to identify the main phenomenological effects of CNT on the amperometric biosensing in order to provide a useful approach still required because "questions remain regarding the fundamental electrochemical properties of CNTs, that need to be resolved for the field to advance in a rational manner"[41]. The aim of the paper is to also show how these effects may be used to extensively study the role of carbon nanotubes in electrochemical biosensing. In this paper, the main equations usually considered in electrochemistry are used to introduce three main effects; these effects are then defined, evaluated in several cases, and finally used to prove that different redox processes can manifest completely different effects when occurring at the surface of the same kind of carbon nanotubes.

2. Experimental

2.1. Chemicals

Carbon paste *Screen-Printed Electrodes* (SPE, model DRP-100) and MWCNTs were purchased by Dropsens (Spain). The electrodes consist of graphite working electrode (4 mm diameter), graphite counter electrode, and Ag/AgCl reference electrode. MWCNT (10 nm diameter, 1-2 μm length) were purchased in powder (90% purity) by Dropsens (Spain), and subsequently diluted in chloroform to the concentration of 1 mg/ml [30]. Samples were then sonicated in order to obtain a homogeneous solution. Hydrogen peroxide (H_2O_2) was purchased from Reactolab SA (Switzerland), while ferricyanide was supplied by Riedel de-Haën (Switzerland).

The microsomal cytochrome P450 3A4 (Sigma-Aldrich, Switzerland) and microsomal cytochrome P450 2B6 (BD Bioscience, USA) were purchased as isozyme microsomes with recombinant human cytochrome (CYP3A4 or CYP2B6), recombinant NADPH-P450 reductase, and cytochrome b_5, expressed in baculovirus infected insect cells. Microsomes provided in 0.1 M of *Phosphate Buffer Saline* (PBS, from Sigma-Aldrich) at pH 7.4, were used as received. Milli-Q water (18 MW/cm) was used to prepare all aqueous solutions. All experiments were carried out in a 0.1 M PBS solution (pH 7.4) as supporting electrolyte. The drugs cyclophosphamide and ifosfamide were purchased in powder from Sigma-Aldrich, and dissolved in Milli-Q water, before storing at 4 °C. Etoposide was again from Sigma Aldrich but it was dissolved in *dimethyl sulfoxide* (DMSO) due to its low solubility in water.

2.2. Electrodes preparation

SPE were functionalized with MWCNTs according to [44]. A solution of 30 μl of MWCNT-chloroform was gradually casted (in small aliquots of 2 μl) on the working electrode. Between two sequential depositions, the chloroform evaporated and the nanotubes formed a three-dimensional nanostructured network at the electrode surface.

For detection of drugs, MWCNT-SPE were further functionalized with microsomal cytochrome P450: isoforms 2B6 and 3A4 for detection of both ifosfamide and cyclophosphamide. Three drops of cytochrome P450 (9 ml each drop), were subsequently applied in order to generate homogeneous layers of protein on the nano-structured working electrode, before being stored at 4 °C overnight to promote a homogeneous protein adsorption on the CNT-nanostructure. The excess of cytochrome was then removed by washing with Milli-Q water, and each biosensor was further rinsed in Milli-Q water before each measurement. All the functionalized electrodes were stored in PBS at 4 °C until use.

2.3. Electrochemical measurements

The electrochemical response of electrodes was investigated by cyclic voltammetry (CV) and chronoamperometry under aerobic conditions. Electrochemical measurements were acquired by using an Autolab potentiostat (Metrohm, The Netherlands). For cyclic voltammetry, the electrochemical cell was covered with 100 μl drop of solution containing hydrogen peroxide, ferricyanide, or drugs (etoposide, cyclophosphamide or ifosfamide) at different concentrations diluted in 0.1 M PBS at pH 7.4. Then, the potential is swept within the range from -300 mV to +700 mV, from -1000 to +1000 mV, or from -600 to +300 mV for ferricyanide, hydrogen peroxide and drugs, respectively. For chronoamperometry, the screen-printed electrode was instead immersed into a volume of 25 ml of PBS solution under stirring conditions. A volume of 25 μl of the target molecule was successively added per step into the solution every 400 s. All the electrochemical measures were acquired at room temperature.

Calibration curves were obtained by plotting the Faradaic current (current steps for chronoamperometry and current peak for cyclic voltammetry) *vs.* concentration of the target molecule. The sensitivity was computed as the slope of the calibration curve [45]:

$$\bar{S} = \frac{\Delta I_F}{\Delta C}, \tag{1}$$

Of course, the sensitivity per unit of area is:

$$S = \frac{\Delta I_F}{A\Delta C}, \tag{1'}$$

The *Limit of Detection* (LOD) was computed, as usual, from the baseline noise according to the expression[45]:

$$LOD = \sigma\frac{\delta i}{S}, \tag{2}$$

where δi is the standard deviation of the blank measurements, S is the sensitivity by Equation (1), and k is a parameter accounting for the confidence level (σ = 1, 2, or 3 corresponds to 68.2%, 95.4%, or 99.6% of statistical confidence). Both the sensitivity and limit of detection were evaluated within the linear range of each calibration curve.

2.4. SEM imaging

Morphological analysis of bare, structured and functionalized electrodes was done by using a Philips/FEI XL-30F microscope (Eindhoven, The Netherlands) to acquire *Scanning Electron microscopy* (SEM) images. The scanning electron microscope was operated in 1.5–4.2 mm ultra-high resolution mode. The nominal resolution was 2.5 nm at 1 kV.

3. Results and Discussion

3.1. Electron Transfer mediated by carbon nanotubes

The sentence that the "use of carbon nanotubes, as the conductive part of the composite, facilitated fast electron transfer rates" [25] refers to their extraordinary electrical properties (*e.g.*, the mean free path reaches several tens of μm in MWCNT [46]), which are noteworthy but not sufficient to explain their role in biosensing. The key point here is the electron exchange between the CNT and the electrochemical system and not only the *Electron Transfer* (ET) within the tube. The ET from the tube to the molecule under the redox process can be modeled with the perturbation theory. In non-adiabatic reactions, quantum mechanics shows that the ET rate is then [47]:

$$k_{ET} = \frac{2\pi}{\hbar} V_T^2 FC \tag{3}$$

where $V^2{}_T$ is the electronic coupling between the redox molecule and the CNT, *FC* is the Franc-Condon weighted states-density, and *h* is the Plank constant. The *FC* term is the integrated overlap of the wave functions of electrons in the Lowest-Unoccupied-Molecular-Orbital (LUMO) of the redox molecule and the Fermi level of the electrons sea in the CNT. *FC* may be computed as [47]:

$$FC = \frac{1}{\sqrt{4\pi\lambda kT}} e^{-\left(\lambda kT\sqrt{-\Delta G^0 - \lambda}\right)} \tag{4}$$

with **λ** as the increased polarity of the redox center, $\Delta \boldsymbol{G^0}$ as the Gibbs Free Energy corresponding to the ET process, *k* as the Boltzmann constant, and T as the temperature. $V^2{}_T$ is related to the tunneling distance *d* [47]:

$$V_T^2 = V_0^2 e^{-\beta(\phi)d} \tag{5}$$

V_0 is the coupling at null distance, and $\beta(\phi)$ is the decay function that depends, in general, by the tunneling barrier ϕ.

However, it is extremely difficult to investigate the redox processes occurring in CNT biosensors by taking into account the Equations (3)-(5) because of the complexity of the ET transfer chain usually involved in the sensor. Let us consider, for example, the case of a cytochrome: in this enzyme, the redox reaction occurs at the HEME active site of the protein [48]. Here, electrons move from the oxidized substrate to the HEME in agreement with Equation (3). The collected electrons flow from the HEME to the external surface of the enzyme via long-range electronic interactions supported by overlapping molecular segments [49], *e.g.* the residues of the enzyme. Then, electrons jump from the protein to the CNT again in accordance with Equation (3). On the CNT, electrons flow by following the ballistic conductivity [17] and, once reached the interface between the tube and the WE, they can enter the Fermi level in the metal, once again with the mechanism described by Equation (3). In conclusion, the electron flow from the oxidized species to the electrode follows an extremely complex chain of ETs, where each step is governed by different ET rates, making the whole chain extremely hard to be correctly modeled. Therefore, a rigorous theoretical approach starting from quantum principles is not feasible with respect the present stat-of-the-art in molecular computation.

3.2. Sensitivity and Detection Limit with carbon nanotubes

SPE made of carbon-paste are usually considered for applications in electrochemical biosensing. They present a rough surface with features having typical size in the range from 10 to 50 nm, as shown in Fig. 1(A). Such a surface proves to be especially successful when dealing with electrochemical biosensing, *e.g.* for glucose detection. There are mainly two reasons for this: their features in the scale of tens of nanometers are suitable to accommodate probe-proteins, which are typically in the range of 5-10 nm, and the carbon-based materials present a good affinity with hydrogen peroxide [50] that allows for a large ET.

This last is important because all the biosensors based on enzymes form the family of oxidases collect electrons released during the redox reaction of hydrogen peroxide [51]:

$$H_2O_2 \overset{+650mV}{\longrightarrow} 2H^+ + O_2 + 2e^-, \tag{6}$$

while the hydrogen peroxide is produced in the catalysis of the enzyme's substrate:

$$Glu + O_2 \overset{GOD}{\longrightarrow} Glu.Acid + H_2O_2 \tag{7}$$

Equation (7) is written for the D-glucose - *Glu*- transformed in D-gluconic Acid δ-lactone–*Glu.Acid* - but similar equations are valid for several other endogenous metabolites catalyzed by proper oxidases.

In these cases, the affinity is even further improved by impurities usually present on CNT. In fact, iron impurities from the fabrication processes of CNT are observed to be the active sites of the electrochemical reduction of hydrogen peroxide [52]. Of course, variations between different batches of CNTs from the same manufacturer, or between different manufacturers, definitely affect the electrode response. So, we need to consider that when studying the general response of hydrogen peroxide. For this reason, we have paid special attention in this research to use only one supplier for both screen-printed electrode and CNT (Dropsens from Spain) and to use mainly CNT from the same branch of production.

We would like now to address not only the case of oxidases, but also more in general the electrochemical detection based on enzymes different than oxidases. We will show in the following of the paper that we have obtained very different effects of CNT on very different electrochemical systems. The main goal of the paper is, then, to compare different biological systems that provide electrochemical biosensing by using the very same nanostructured electrodes. For this reason, we will not stop with the discussion on the active sites for the electrochemical reduction of hydrogen peroxide, but we will proceed to introduce a more general phenomenological approach that works in all the cases.

As already mentioned, a nanostructured surface improves the active electrochemical area and, thus, the total amount of the collected current:

$$I_F = A j_F, \tag{8}$$

with respect to the same amount of Faradaic current density j_F. In principle, a larger total current related to Faradaic processes at the surface means a larger signal-to-noise ratio. Equation (2) proves that a larger signal-to-noise ratio returns a smaller limit of detection and, therefore, it proves that the electrochemical sensor is

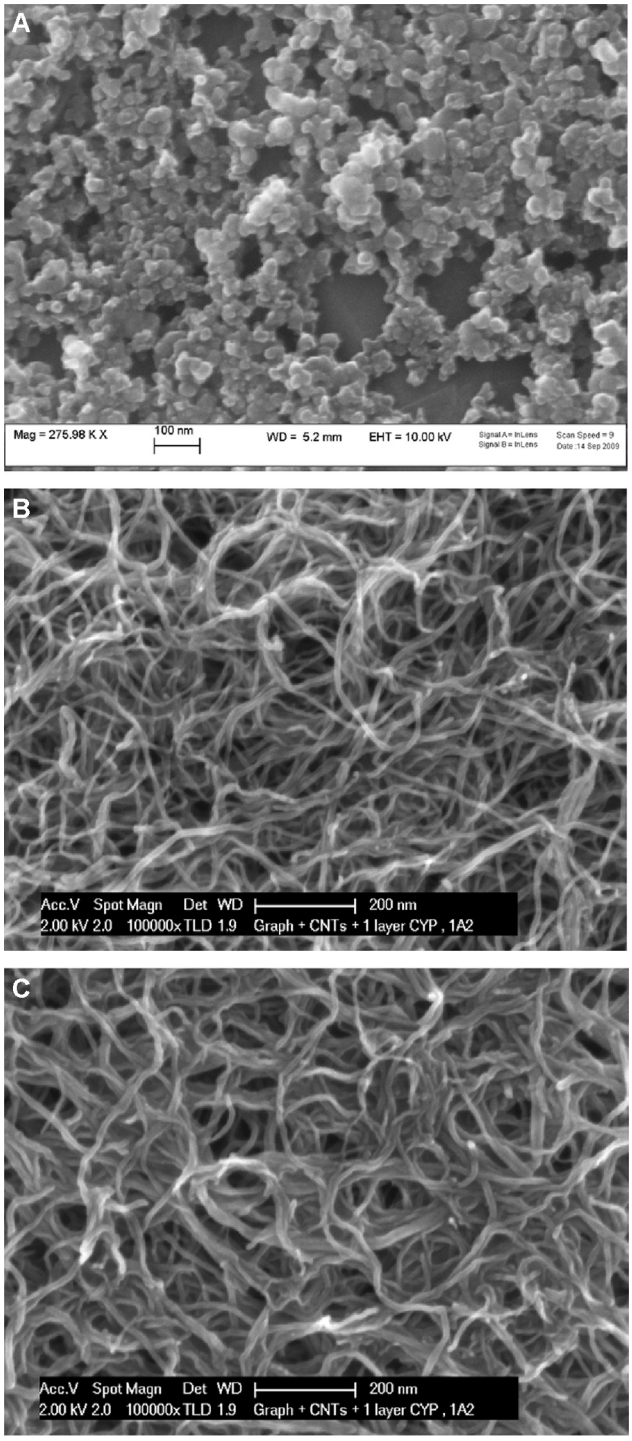

Fig. 1. SEM images of screen-printed electrodes bare (A), nanostructured with carbon nanotubes (B), bio-functionalized with cytochromes P450 (C).

sensitive for smaller quantities. However, Equation (1′) shows that the sensitivity per unit of area is independent by the active electrochemical area because Equation (8) has a direct relationship with A:

$$S = \frac{\Delta j_F}{\Delta C} \tag{9}$$

Equation (9) shows that the sensitivity per unit of area is only related to the current density and not to the total one. Therefore, the sensitivity of an electrochemical sensor appears to be, in principle, independent from the SPE nano-structuring. According to Equation (8), the LOD is also independent from the area A:

$$LOD = \sigma \frac{\delta i}{A \Delta j_F} \Delta C = \sigma \frac{\delta j_{blank}}{\Delta j_F} \Delta C \tag{10}$$

Because the standard deviation of the blank measurements (δi) is the total current collected at the WE, this includes the area of the electrode. Equation (10) reminds us that the LOD is a concentration (the minimum detectable one). The LOD is then defined by the minimum amount of Faradaic current density that overcomes the standard deviation of the current density in the blank measures (δj_{blank}). Therefore, also the LOD of an electrochemical sensor appears to be, in principle, independent from the SPE structuring with further nano-materials. However, this is not exactly true for almost all the considered chemical species, as it is shown in the following sections. In the following, we will explain also why *S* and *LOD* look (erroneously) independent from the increased area due to nano-structuring.

Among several different approaches for depositing carbon nanotubes, which also include microspotting [53], electrodeposition [54] and the direct growth [33,55], we simply used the drop casting [44]. While microspotting, electrodeposition and direct growth enable a more precise localization of CNT on the working electrode, it has been shown that drop casting may further extend the electro-active area by creating a sort of conducting CNT forest in the insulating area surrounding the WE [56]. Also for this reason, we decided to use the drop casting technique in this study.

Fig. 1(B) shows the result obtained on a SPE further structured by using MWCNT. The used CNT have a mean diameter of 10 nm and create a densely packed network (as shown in the SEM image). The obtained surface now presents a higher surface convolution that further increases the collected total current as described by Equation (8). Moreover, the surface now structured with MWCNT accommodates even more protein as due to the increased available binding sites. The CNT create a natural forest for hosting more proteins thanks to the hydrophobic character of their walls [35]. Fig. 1(C) clearly shows that the proteins create a homogeneous biological-layer surrounding all the tubes. The fiber-like features in Fig. 1(C) are clearly larger in diameter than those in Fig. 1(B). That is due to biological molecules absorbed all around the MWCNT. Similar increases of the CNT diameter after functionalization have been registered several times, *e.g.* in both the case of oxidases [57], and cytochromes [35]. It has been demonstrated that this increase closely corresponds to the protein size [44] and it was confirmed by more precise Monte Carlo simulations[35]. Simulations have also shown that the protein adsorption is due to the hydrophobic interactions between the external surface of sidewall of MWCNT and protein' residues that manifest hydrophobic character [35].

3.3. Cottrell effect

Equation (8) says that we can obtain larger signal-to-noise ratios by larger active electrochemical areas. However, Equations (9) and (10) do not confirm that we could have more sensitive sensors. The only way to improve the sensor sensitivity is to increase the current density in Equations (9) and (10). We can also see the same in a different way. It is well known in electrochemistry that we can use the so-called ***Cottrell equation*** when using electrochemical sensors driven with a fixed potential. The Cottrell equation relates the total collected Faradaic current with the concentration of redox species [58]:

$$I_F(t) = \frac{nFA\sqrt{D}}{\sqrt{\pi t}} C(t) \tag{11}$$

Equation (11) describes the variation in time of the Faradaic current collected at the WE with area *A*, and related to a redox species at

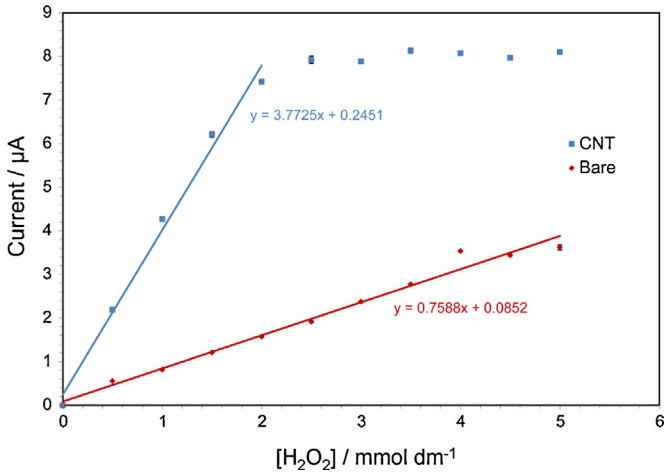

Fig. 2. Calibration curves showing the Cottrell effect.

the concentration $C(t)$ that has a diffusion coefficient D and releases n electrons (F is the Faraday constant). By definition, Equation (11) defines the so-called "chronoamperometry". By Equation (11), we clearly see that the sensitivity does not depend on the active area:

$$S = \frac{nF\sqrt{D}}{\sqrt{\pi t}} \tag{12}$$

However, the derivation of Equation (12) is actually wrong. The reason is that we always consider "the geometrical area" (A_g) of our SPE substrates when performing the computation in Equation (1′). In opposite, the area that appears now in Equation (11) is the "electrochemical active surface area" that receives a contribution from CNT (A_{CNT}). By taking into account these two different areas, the Equation (12) is more conveniently written as:

$$S = \frac{nF(A_g + A_{CNT})\sqrt{D}}{A_g\sqrt{\pi t}} \tag{13}$$

Now, the right version of the sensitivity per unit of area as computed by the Cottrell equation shows that a SPE for chronoamperometry may get benefit out of structuring with CNT.

Cottrell equation, and then Equation (13), applies to diffusion-only redox reactions [59]. As seen before, there is a diffusion layer in the region around carbon nanotubes that does not necessarily support phenomena following the semi-infinite planar diffusion model [42]. Even more complex are the cases when the enzyme directly exchanges electrons with the CNT (as in the case of cytochromes P450). In these cases, the ET rate is increased by CNT edge-planes [36,37] as well as by the number of metal/metal oxide impurities [39] in the tubes. However, many quasi-reversible systems show straight-line plots of Faradic current versus concentration similarly to what is seen in Equation (11). Therefore, now it is straightforward to generalize the concept and introduce the following definition related to the increase of sensitivity due to CNT without necessarily referring to diffusion-only redox reactions.

Definition

We define Cottrell effect as the increase in sensitivity per unit of area as observed in chronoamperometry and due to nano-structuring of the electrodes.

The LOD by Equation (2) decreases as well because S is computed with Equation (13). Back to the case of hydrogen peroxide described in (6), we find confirmation of the *Cottrell effect* in Fig. 2: the reported data correspond to a limited sensitivity per unit area equal to 5.5 ± 1.4 μA/mM ×cm^2 for the calibration on bare SPE, while the sensitivity increases to 28.1 ± 9.8 μA/mM ×cm^2 on MWCNT electrodes. The *Cottrell effect* is here about a factor 5x, which is coherent with other similar values previously obtained on the same kind of structured SPE [60]. The sensitivity for hydrogen peroxide detection has also been ameliorated up to 70.7 μA/mM ×cm^2 by immobilizing the peroxidase on glassy carbon electrodes structured with MWCNT embedded in chitosan polymer [32]. Of course, the *Cottrell effect* on hydrogen peroxide is transferred on all the sensing systems based on catalytic processes similar to (7): the sensitivity increases on MWCNT up to 27.7, 35.6, 2.7 and 0.1 (all in μA/mM ×cm^2) for glucose [57], lactate [51], ATP [31], and cholesterol [26], respectively. To confirm the role of A_{CNT} in Equation (13), some Monte-Carlo simulations performed by using the Fowler–Nordheim theory on electrons extraction from drop-casted CNT have demonstrated that the larger contribution to electrochemical bio-sensing comes from the sidewall of the tubes [61] although side-walls present very slow ET rates per unit area [27]. Studies on SWNTs have confirmed that the sidewall might have much more electrochemical activity than expected [62].

Fig. 2 shows that ET from hydrogen peroxide is much more efficient on MWCNT than on bare SPE. However, it seems that the MWCNT are not so powerful for all the redox reactions occurring at their surface. The case of ferricyanide is quite significant. Any search in literature for the electrochemical detection of ferricyanide as powered by CNT returns only very few articles. And these articles show a minute amount of advancement. For example, the sensitivity varied only from 62.8 ± 0.3 to 71.5 ± 0.3 μA/mM × cm^2 in case of differently oriented MWCNT [33], while *Cottrell effect* results in 9 times larger sensitivity by varying the MWCNT orientation on hydrogen peroxide [63]. It is worth noting that these last-mentioned experiments on ferricyanide have been conducted on MWCNT directly grown on silicon substrates while it is hard to find literature on ferricyanide detection done by using MWCNT drop-casted on SPE. In our direct measurements, chronoamperometry measures on ferricyanide did not result in any augmentation of the collected current although acquired on SPE structured with drop-casted MWCNT. For ferricyanide, Equation (13) does not work.

3.4. Randle-Sevčick effect

Redox reactions described by Equations (6) and (7) also generate Faradaic current in experiments with voltage scan across the value of +650 mV. If the potential is varied in a cyclic manner, a Faradaic current is registered any time the cyclic voltammogram passes through the value of +650 mV. It is well known in electrochemistry that the maximum peak current collected at the electrode is then related to the redox-species concentration by means of the so-called ***Randle-Sevčick equation*** [58]:

$$I_F \propto nFA\sqrt{\frac{nFD\upsilon}{RT}}C \tag{14}$$

Now, the voltage scan-rate υ, the gas constant R, and the sample temperature T are present in the formula as well.

As we did before for chronoamperometry, we can use Equation (1) and compute the sensitivity per unit area in cyclic-voltammetry by distinguishing the electrochemical active surface area by the geometrical one:

$$S = \frac{nF(A_g + A_{CNT})}{A_g}\sqrt{\frac{nFD\upsilon}{RT}} \tag{15}$$

Equation (15) is now slightly different from Equation (13), but we can easily see a similar increase in sensitivity and a consequent decrease in LOD by structuring with CNT.

As we have seen for the Cottrell equation, Randle-Sevčick analysis also applies only to truly reversible kinetics or truly irreversible ones [58] while most systems, some chosen for this study, are quasi-reversible. Therefore, we generalize here the concept and introduce

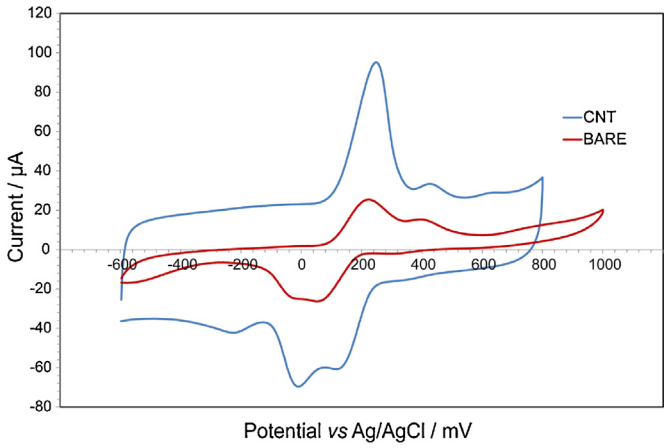

Fig. 3. Calibration curves showing clear Randle-Sevčick effect on the direct detection of Etoposide (250 µM).

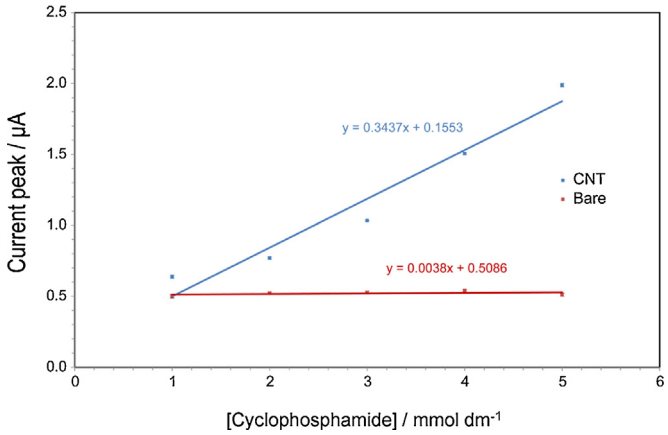

Fig. 4. Calibration curves showing a clear Randle-Sevčick effect on Cyclophosphamide as detected by the Cytochrome P450 2B6.

the following definition related to the increase of sensitivity due to CNT without necessarily referring to diffusion-only redox reactions.

Definition

We define Randle-Sevčick effect as the increase in sensitivity per unit of area observed in cyclic voltammetry due to nano-structuring of the electrodes.

The *Randle-Sevčick effect* has been already demonstrated in literature for oxidases-based sensors in the detection of glucose [24], lactate [28], cholesterol [30], and thiocholine [27]. The *Randle-Sevčick effect* was also registered in several other redox systems. Fig. 3 shows the *Randle-Sevčick effect* on all the redox peaks present in the direct hydrolysis of another relevant molecule: the etoposide. Etoposide is a well-known anti-cancer agent that is highly electrochemically active. A series of ETs related to redox reactions related to his molecular components are clearly observable even on bare SPE (Fig. 3). All these Faradaic currents are greatly increased when the etoposide is reduced onto MWCNT, as shown by the higher peaks in Fig. 3. In our experiments, an increase in sensitivity equal to 2.30 ± 0.33 µA/mM $\times$cm^2 on MWCNT electrodes has been registered, while it was found to be limited to 0.29 ± 0.03 µA/mM $\times$cm^2 on bare SPE.

The *Randle-Sevčick effect* is registered in detection based on enzymes other than oxidases, as well. The class of cytochromes P450 is a class of enzymes that catalyze most of the commonly used drugs [54]. The drugs transformation from their native state (RH) to an oxidized one (ROH) occurs in nature by the presence of a co-enzyme called NADPH (the reduced form of Nicotinamide Adenine Dinucleotide Phosphate Phosphate):

$$RH + O_2 + H^+ + NADPH \xrightarrow{P450} ROH + NADP^+ + H_2O, \quad (16)$$

Whereas, in water solutions transformation may occur without NADPH if electrons are supplied by SPE where the P450 is immobilized [53]:

$$RH + O_2 + 2H^+ + 2e^- \xrightarrow{P450} ROH + H_2O \quad (17)$$

Equation (17) shows electrons coming from the electrodes in a similar way that Equation (6) shows electrons released to the electrodes. Fig. 4 shows that the sensitivity related to Equation (17) may be enhanced as well as the sensitivity registered in reaction following Equation (6). The Figure shows the detection of the cyclophosphamide (a well-known anti-cancer drug) as detected by the Cytochrome P450 2B6. The detection of 5 mM of cyclophosphamide is practically negligible when the protein is immobilized on bare SPE. The detection of 5 mM of that drug results indeed in a large current, up to almost 2 µA, when the protein is immobilized on SPE structured with MWCNT. Table 1 shows that the registered current is always around 0.5 µA with bare SPE while, as seen in the calibrations curve, it goes up to 1.99 µA with MWCNT. It corresponds to an enhanced sensitivity computed in 2488 µA/mM $\times$cm^2. Similarly, sensitivities of 120 and 880 µA/mM $\times$ cm^2 have been registered for Ifosfamide and Ftorafur [35] (two other anti-cancer drugs) while 25 µA/mM $\times$cm^2 have been registered for Naproxen [44] (an anti-inflammatory compound). MWCNT have been also used to quantify NADH (Nicotinamide Adenine Dinucleotide) and have shown clear *Randle-Sevčick effect* with Faradaic currents increase by 20-fold [64].

3.5. Nernst effect

Table 1 also shows another effect: the Faradaic peaks related to the redox of cyclophosphamide are located close to 299 ± 2 mV on the SPE electrode. However, the peaks shift toward smaller potentials when the protein is immobilized onto MWCNT. The peaks are now located in between 248 and 285 mV, depending on the drug concentration. In the case of cyclophosphamide at 5 mM, we get the redox on CNT by saving 50 mV, which is not a negligible saving. This diminished-potential means less energy in the ET, *e.g.* it means less voltage in designing proper electronics to drive this interface. Two clear extra-advantages in using MWCNT in the electrochemical interface. In electrochemistry, the position (E) of the redox and oxidation peaks of a species is related to the standard potential (E_0) and to the concentration of the species in oxidized and reduced forms by the well-known ***Nernst equation*** [58]

$$E = E_0 + \frac{RT}{nF} \ln \left[\frac{C_o}{C_R} \right] \quad (18)$$

However, we cannot simply use the semi-infinite planar diffusion model [59] when dealing with nano-structuring. In this case, the phenomenon is more accurately explained by thin-layer effects, which can have a profound impact on the observed peaks potential and separation. In fact, the following equation was proposed for a fully irreversible electron transfer system [42]:

$$E = E_{Nerst} + \frac{ET}{\alpha F} \ln \left(\frac{\alpha F \upsilon}{RTlk_0} \right), \quad (19)$$

Where E_{Nerst} is the potential given by Equation (18), l is the thickness of the thin layer, α and k_0 are the usual transfer coefficient and standard heterogeneous rate constant, respectively[58]. As explained [42], less time is required to deplete the layer of electro-active species because we are now facing only a layer of thickness l and, therefore, the peak shifts to less oxidative potentials.

Table 1
Randle-Sevcick effect and clear Nernst effect on Cyclophosphamide by P450 2B6.

Cyclophosphamide Concentration	Bare		CNT	
	Current (μA)	*Potential (mV)*	*Current (μA)*	*Potential (mV)*
1 mM	0.51 ± 0.01	-302.1 ± 1.9	0.64 ± 0.01	-285.0 ± 3.8
2 mM	0.50 ± 0.01	-299.7 ± 1.9	0.77 ± 0.00	-280.1 ± 1.1
3 mM	0.52 ± 0.01	-294.8 ± 1.7	1.03 ± 0.01	-265.5 ± 3.6
4 mM	0.53 ± 0.01	-299.7 ± 2.0	1.51 ± 0.01	-265.5 ± 3.8
5 mM	0.51 ± 0.01	-298.5 ± 2.6	1.99+0.01	-248.4 ± 3.6

Table 2
Randle-Sevčick effect and clear Nernst effect on Cyclophosphamide by P450 3A4.

Cyclophosphamide Concentration	Bare		CNT	
	Current (μA)	*Potential (mV)*	*Current (μA)*	*Potential (mV)*
1 mM	0.82±0.01	-288.6±3.8	1.54±0.01	-221.1 ± 7.7
2 mM	0.82±0.01	-279.7±2.8	1.59±0.02	-220.5 ± 8.7
3 mM	0.84±0.01	-272.7±3.1	1.60±0.01	-222.1 ± 7.3
4 mM	0.86±0.01	-264.4±2.9	2.12±0.01	-225.7 ± 4.6
5 mM	0.85±0.01	-262 2±3 1	3 02±0.01	-223.6 ± 4.6

Table 3
Largely evident Nernst effect on H_2O_2.

H_2O_2 Concentration	Bare		CNT	
	Current (μA)	*Potential (mV)*	*Current (μA)*	*Potential (mV)*
10 mM	3.9 ± 0 1	706±0.4	9.1+1.6	174 ± 2.7
20 mM	23.7 ± 0.1	682±0.3	37.0 ± 1.9	204 ± 0.8
30 mM	49.5 ± 0.2	665±0.3	70.5 ± 1.3	230 ± 0.8
40 mM	55.0 ± 0.2	623±0.4	103.5 ± 2.4	291 ± 0.5
50 mM	64.4 ± 0.3	572±0.3	115.0 ± 2.7	284 ± 0.5

However, different shifts in potential have been observed in using the same nanostructuration in combination with apparently very similar redox systems. Coherently with Equation (19), a clear shift toward less oxidative potentials is clearly observed on hydrogen peroxide (see Table 3) while no shift is observed in the case of ferricyanide (see Table 4). Even more interesting is to note that apparently similar redox reactions catalyzed by the same enzyme give opposite shifts: the same cytochrome P450 3A4 shows less oxidative potential in the case of Cyclophosphamide (see Table 2) while it shows more oxidative potential in the case of Ifosfamide (see Table 5).

Once again, this analysis strictly applies only to truly reversible and truly irreversible kinetics [58] while most systems present quasi-reversible kinetics. Therefore, the definition of an effect operated by nano-structuring on the position of Faradic peaks may help in characterizing and comparing the obtained gain by CNT.

Definition

We define Nernst effect the peak shift as resulting in cyclic voltammetry and due to nano-structuring of the electrodes.

The *Nernst effect* has been already registered several times on many different electrochemical systems, such as for glucose [65], on differently oriented MWCNT [63], and on mixtures involving both dopamine and ascorbic acid [66,67]. The *Nernst effect* has also been exploited to discriminate four different but usually overlapping redox molecules: ascorbic acid, dopamine, uric acid and nitrite [68].

In our results, we have directly observed a clear *Nernst effect* on cyclophosphamide also when detected by another isoform of the same cytochrome: the 3A4 (Table 2). At 5 mM of cyclophosphamide, we saved here almost 40 mV. We have also observed a much more evident *Nernst effect* on hydrogen peroxide (Table 3). Here the effect of MWCNT is extremely high: we got saving up to 532 mV for 10 mM of H_2O_2. Fig. 5 represents the situation even better: we have a lot of voltage saving by structuring SPE with MWCNT, when dealing with hydrogen peroxide. That means CNT are much more effective in providing voltage savings when dealing with molecules like hydrogen peroxide rather than dealing with a molecules like cyclophosphamide. Cyclophosphamide is detected through protein mediators such as the cytochromes P450 3A4 or 2B6. The two electrochemical-systems are actually so different that it is not right to compare each other. The hydrogen peroxide is an extremely small molecule (just little bigger than a water molecule) that goes through a direct redox onto the electrodes surface. The cyclophosphamide is also a small molecule, but the interface contains now an extremely huge molecule (the cytochromes P450 is a 50kDa (kilodaltons) protein) that hosts for a while cyclophosphamide in its HEME group. The HEME is located in the enzyme active site. So,

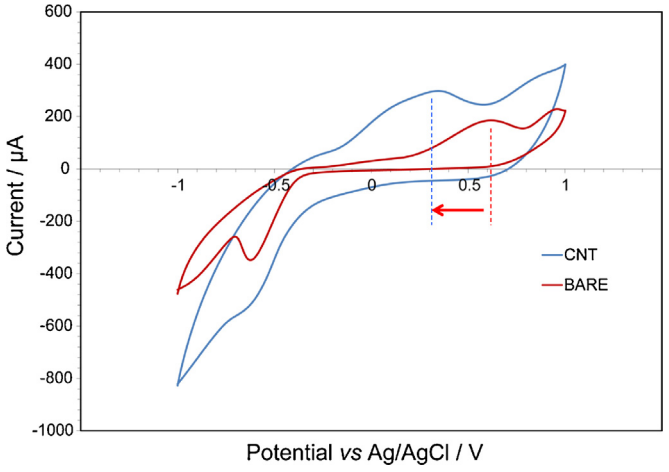

Fig. 5. Cyclic voltammograms showing clear Nernst effect on hydrogen peroxide (at concentration 50 mM).

Table 4
Neither Randle-Sevčick effect nor Nernst effect on Ferricyanide.

Ferricyanide Concentration	Bare		CNT	
	Current (μA)	*Potential (mV)*	*Current* (μA)	*Potential (mV)*
2.5 mM	51.8 ± 0.1	184±0.4	41.8 ± 0.2	205 ± 1.2
5 mM	80.8 ± 0.1	235±0.4	68.9 ± 0.2	236 ± 1.2
10 mM	165.4 ± 0.3	276±0.4	141.0 ± 0.5	271 ± 3.1
15 mM	245.8 ± 0.5	309±0.4	207.6 ± 0.8	298 ± 0.2
20 mM	309.2 ± 0.8	337±0.3	273.7 ± 1.1	318 ± 0.4

Table 5
Opposite Nernst effect (and Randle-Sevčick effect) on Ifosfamide by P450 3A4.

Ifosfamide Concentration	Bare		CNT	
	Current (μA)	*Potential (mV)*	*Current* (μA)	*Potential (mV)*
1 mM	0.76±0.01	-245.7 ± 4.1	0.44±0.01	-267.1 ± 9.1
2 mM	0.79±0.01	-240.1 ± 3.3	0.56±0.01	-255.5 ± 8.3
3 mM	0.82±0.01	-231.3 ± 3.3	0.86±0.01	-239.5 ± 6.2
4 mM	0.87±0.01	-227.6 ± 2.7	1.38±0.01	-240.5 ± 6.1
5 mM	0.88±0.01	-225.7 ± 3.4	2.01±0.01	-238.6 ± 5.6
6 mM	0.86±0.02	-224.2 ± 4.5	2.55±0.02	-240.8 ± 6.1

the cytochrome needs to bring electrons out of the electrode's surface and transport them till its HEME through long-range electronic interactions supported by overlapping LUMO orbitals in adjacent enzyme residues [49]. Therefore, it will not be so surprising to get more obvious *Nernst effects* on very small molecules and a smaller effect on extremely complex ET chains. However, this simple explanation does not work because many other interesting features of the *Nernst effect* are registered on apparently very similar systems.

Worth of note is that cyclophosphamide on 2B6 goes up in voltage-savings by increasing the concentration (Table 1) while hydrogen peroxide goes down in saving by increasing the concentration (Table 3). Taking into account that different concentrations change the peak locations even on bare SPE, we can see that *Nernst effect* becomes less evident once the concentration increases. From 10 mM to 50 mM of H_2O_2, the advantage on the *Nernst effect* by MWCNT decreases by 46%, and from 1 m M to 5 mM of cyclophosphamide, the *Nernst effect* decreases by 42% in the interaction with 3A4 (Table 2). That is a very similar gain loss. However, the two decreases are determined by two different behaviors of the systems: the H_2O_2 shows a redox peak that decreases with concentration on SPE while increases on MWCNT. The cyclophosphamide on 3A4 shows a redox peak that decreases with concentration on SPE while did not shift on MWCNT: the peak position is always located at 222 ± 7 mV. Even more differently, the cyclophosphamide on 2B6 shows a peak going down with concentration on MWCNT (Table 1). In the latter case, the cyclophosphamide shows opposite behavior with respect to H_2O_2!

So, we have here the same phenomenon when dealing with bare SPE for all the three considered systems: H_2O_2, cyclophosphamide on both 2B6 and 3A4 show a *Nernst effect* with increased potential at increased concentrations. While we have three different *Nernst effects* when dealing with MWCNT: H_2O_2 shows a peak that goes up with concentration, cyclophosphamide on 3A4 presents a peak that does not shift, and cyclophosphamide on 2B6 has a peak that goes down.

And that is not the only "non-coherent" behavior we might find by looking for the *Nernst effect* with CNT. Table 4 shows that the ferricyanide is very slightly affected by the *Nernst effect*: the peak location is slightly increasing with the concentration in both the case of SPE and MWCNT. For the concentration at 5 mM, the peak location is statistically identical (at 235 ± 1.2 mV) in both cases, while for the other concentrations the difference in peak location is never larger than 10 mV. Table 4 also shows that the ferricyanide does not take advantage by CNT neither in relation to the *Randle-Sevčick effect*: the total Faradaic currents registered on ferricyanide on both SPE and MWCNT are again very close to each other. The table even shows we actually collect more current on SPE than on MWCNT. This fact contradicts Equation (15). So, we have to conclude that, again, Equation (15) does not work for ferricyanide. The only explanation is that we still do not have a fully understood and complete theory that could take into account the role of CNT. Fig. 6 summarizes quite well the situation on ferricyanide: the voltammograms are extremely similar, with peaks of very close amplitudes and voltage-locations, for both SPE and MWCNT. We have found this kind of very-similar behavior for several series of experiments we have done with ferricyanide on MWCNT on SPE electrodes. The conclusion is that the ferricyanide is practically not affected by the presence of CNT in the electrochemical interface, at least when the CNT are drop-cast onto SPE. Another molecule that apparently is not affected by the *Nernst effect* is the etoposide: Fig. 3 shows in fact an extremely clear *Randle-Sevčick effect* but it also shows that the *Nernst effect* is absent. The peaks of etoposide are evidently in almost the same positions on SPE than on MWCNT!

Table 6
Opposite Nernst effect (and Randle-Sevčick effect) on Ifosfamide by P450 2B6.

Ifosfamide Concentration	Bare		CNT	
	Current (μA)	*Potential (mV)*	*Current* (μA)	*Potential (mV)*
1 mM	1.302±0.006	-236.16 ± 2.25	1.141±0.010	-287.08±4.02
2 mM	1.298±0.008	-231.56 ± 2.71	1.178±0.009	-276.96±3.57
3 mM	1.309±0.007	-224.20 ± 2.50	1.203±0.009	-292.29±3.33
4 mM	1.306±0.009	-218.99 ± 2.89	1.212±0.009	-269.59±3.26
5 mM	1.329±0.009	-224.51 ± 2.81	1.477±0.006	-252.73±2.65
6 mM	1.346±0.013	-233.71 ± 3.33	1.698±0.010	-216.84±3.88

Table 7
Sensitivity and Detection limit enhancement on P450 detection.

Drug	Cytochrome P450	Sensitivity (nA/μM*mm^2)		Detection limit (mM)	
		Bare	CNTs	Bare	CNTs
Cyclophosphamide	CYP2B6	2.99+0.50	24.86+0.45	0.856+0.142	0.110+0.002
	CYP3A4	0.87+0.62	37.18+0.73	7.473+5.335	0.084+0.002
Ifosfamide	CYP2B6	0.71+0.05	8.41+0.50	3.870+0.267	0.323+0.019
	CYP3A4	1.87+0.62	35.21+0.69	1.592+0.532	0.086+0.002

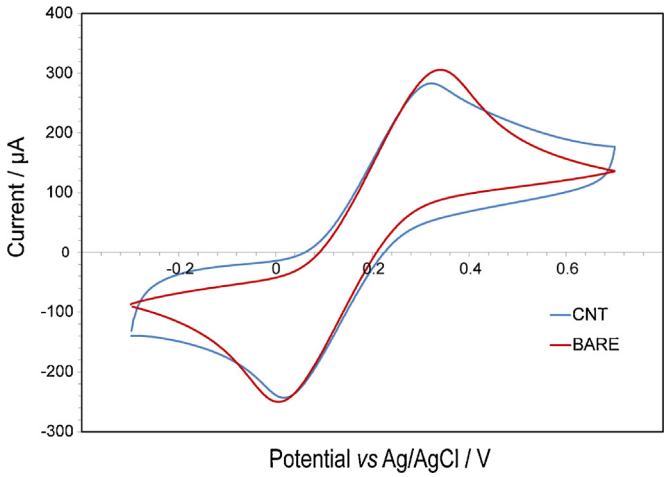

Fig. 6. Cyclic voltammograms showing no Randle-Sevčick neither Nerst effect on Ferricyanide.

On the other hand, the *Nernst effect* has been effectively registered in several electrochemical systems, as we have shown here and as it has been reported several times in literature by other research groups.

Another explanation of how CNT interact with the Nernst effect is that the effective concentration of the reduced and oxidized species at the interface might vary when CNT are involved. In fact, larger layering phenomena are usually registered at the electrochemical interfaces with MWCNT. By using the Electrochemical Impedance Spectroscopy (EIS), it has been already shown several times that the charge-storage capacity increases by almost one order of magnitude when MWCNT are mixed with conductive polymers [69] or when they are electrophoretically deposited on stain-less steel electrodes [70]. This is also coherent with other independent experiments done to demonstrate the ability of CNT to develop super-capacitors [71]. Fig. 3 and Fig. 5 also show clearly more capacitive current on CNT than on bare electrodes. However, this seems to be not reflected on the *Nernst effect* on etoposide. Once again, we have to conclude that we still do not have a complete basic theory that takes into account the full role of CNT (Table 6).

4. Conclusions

This paper has shown that CNT clearly provide great advantages when used in electrochemical biosensing. However, that is not fully true in all the cases and not always works in the same manner. In particular, extra benefits in terms of increased sensitivity and decreased LOD are often registered in electrochemical sensors for both endogenous and exogenous human metabolites. For example, Table 7 summarizes quite well the case of two well-known drug compounds that may be detected by two different probe enzymes. This table actually shows four different bio-sensing systems that all show increased performance in terms of both sensitivity and LOD. In some of the cases, the table shows two orders of magnitude difference in performance gain (*e.g.*, the case of the Ifosfamide as detected by the cytochromes P450 3A4). The basic equations of electrochemistry show us the LOD is apparently independent from the area. Therefore, the LOD values improved by CNT as reported by Table 7 are a further confirmation that the contribution on CNT in electrochemical biosensing is not only due to an increase of the electrochemical active surface area. However, similar benefits are not always registered in all the sensing systems. For example, the detection of ferricyanide does not benefit from further structuring of the working electrodes. In order to investigate the situation better, this paper introduced three effects by considering the basic features of redox processes as investigated with commonly used electrochemical techniques: the *Cottrell*, *Randle-Sevčick* and *Nernst effects*. These effects have been used in this paper to analyze several electrochemical biosensing systems and to demonstrate that the role of CNT depends on the considered redox systems. In particular, we have demonstrated that even in those cases where the CNT make the difference (for example the two drug of Table 7), it might happen that some effects of nano-structuring (*e.g.*, the *Nernst effect*) would be negligible or would result in opposite trends on apparently very similar electrochemical systems. We have also seen that the simple explanation of an increase in electrochemical area works for some cases but faults for others. We have seen that there are several theories, usually supported by experimental verifications that give us a clear appreciation of the various and complex interplay of physico-chemical processes occurring at CNT interface. However, we still have a lot of work to do to fully understand the role of carbon nanotubes in enhancing the performance of electrochemical sensors, especially in the case of semi-reversible electrochemical systems involving enzymes that provide biosensing not mediated by hydrogen peroxide.

Acknowledgments

Authors thank Irene Taurino for useful discussions on the role of Carbon Nanotubes and on the hydrolysis of hydrogen peroxide. The research has been supported by the National SNF Sinergia Project CRSII2 127547/1 and by the International NanoSys Project ERC-2009-AdG-246810.

References

[1] H.P. Boehm, The first observation of carbon nanotubes, Carbon vol. 35 (1997) 581–584.
[2] M. Monthioux, V.L. Kuznetsov, Who should be given the credit for the discovery of carbon nanotubes? Carbon vol. 44 (8) (2006) 1621–1623.
[3] S. Iijima, Helical microtubules of graphitic carbon, Nature vol. 354 (1991) 56–58, 11/07/print.
[4] S. Iijima, T. Ichihashi, Single-shell carbon nanotubes of 1-nm diameter, Nature vol. 363 (1993) 603–605, 06/17/print.
[5] D.S. Bethune, C.H. Klang, M.S. de Vries, G. Gorman, R. Savoy, J. Vazquez, et al., Cobalt-catalysed growth of carbon nanotubes with single-atomic-layer walls, Nature vol. 363 (1993) 605–607, 06/17/print.
[6] L.V. Radushkevich, L.V. O strukt ure ugleroda, obrazujuce gosja pri termiceskom razlozenii okisi ugleroda na zeleznom kontakte, Zurn Fisic Chim vol. 26 (1952) 88–95.
[7] M. Hilbert, N. Lange, The structure of graphite filament, Z. Kristalogr vol. 111 (1958) 24–34.
[8] A. Oberlin, M. Endo, T. Koyama, Filamentous growth of carbon through benzene decomposition, Journal of Crystal Growth vol. 32 (3) (1976) 335–349.

[9] Y. Liu, H. Wang, Nanomedicine: Nanotechnology tackles tumours, Nat Nano vol. 2 (2007) 20–21, 01//print.
[10] J.A. Hubbell, A. Chilkoti, Nanomaterials for Drug Delivery, Science vol. 337 (2012) 303–305, July 20, 2012.
[11] W.A. de Heer, A. Châtelain, D. Ugarte, A Carbon Nanotube Field-Emission Electron Source, Science vol. 270 (1995) 1179–1180, November 17, 1995.
[12] H.D. Wagner, Nanocomposites: Paving the way to stronger materials, Nat Nano vol. 2 (2007) 742–744, 12//print.
[13] A.A. Mamedov, N.A. Kotov, M. Prato, D.M. Guldi, J.P. Wicksted, A. Hirsch, Molecular design of strong single-wall carbon nanotube/polyelectrolyte multilayer composites, Nat Mater vol. 1 (2002) 190–194, 11//print.
[14] M.M.J. Treacy, T.W. Ebbesen, J.M. Gibson, Exceptionally high Young's modulus observed for individual carbon nanotubes, Nature vol. 381 (1996) 678–680, 06/20/print.
[15] A.C. Dillon, K.M. Jones, T.A. Bekkedahl, C.H. Kiang, D.S. Bethune, M.J. Heben, Storage of hydrogen in single-walled carbon nanotubes, Nature vol. 386 (1997) 377–379, 03/27/print.
[16] S.J. Tans, M.H. Devoret, H. Dai, A. Thess, R.E. Smalley, L.J. Geerligs, et al., Individual single-wall carbon nanotubes as quantum wires, Nature vol. 386 (1997) 474–477, 04/03/print.
[17] C.T. White, T.N. Todorov, Carbon nanotubes as long ballistic conductors, Nature vol. 393 (1998) 240–242, 05/21/print.
[18] S.J. Tans, C. Dekker, Molecular transistors: Potential modulations along carbon nanotubes, Nature vol. 404 (2000) 834–835, 04/20/print.
[19] A. Modi, N. Koratkar, E. Lass, B. Wei, P.M. Ajayan, Miniaturized gas ionization sensors using carbon nanotubes, Nature vol. 424 (2003) 171–174, 07/10/print.
[20] S. Ghosh, A.K. Sood, N. Kumar, Carbon Nanotube Flow Sensors, Science vol. 299 (2003) 1042–1044, February 14, 2003.
[21] P.W. Barone, S. Baik, D.A. Heller, M.S. Strano, Near-infrared optical sensors based on single-walled carbon nanotubes, Nat Mater vol. 4 (2005) 86–92, 01//print.
[22] D.J. Lipomi, M. Vosgueritchian, B.C.K. Tee, S.L. Hellstrom, J.A. Lee, C.H. Fox, et al., Skin-like pressure and strain sensors based on transparent elastic films of carbon nanotubes, Nat Nano vol. 6 (2011) 788–792, 12//print.
[23] K.A. Williams, P.T.M. Veenhuizen, B.G. de la Torre, R. Eritja, C. Dekker, Nanotechnology: Carbon nanotubes with DNA recognition, Nature vol. 420 (2002) 761, 12/19/print.
[24] A. Guiseppi-Elie, C. Lei, R.H. Baughman, Direct electron transfer of glucose oxidase on carbon nanotubes, Nanotechnology vol. 13 (2002) p559.
[25] V.G. Gavalas, S.A. Law, J. Christopher Ball, R. Andrews, L.G. Bachas, Carbon nanotube aqueous sol-gel composites: enzyme-friendly platforms for the development of stable biosensors, Analytical Biochemistry vol. 329 (2004) 247–252, 6/15/.
[26] G. Li, J.M. Liao, G.Q. Hu, N.Z. Ma, P.J. Wu, Study of carbon nanotube modified biosensor for monitoring total cholesterol in blood, Biosensors and Bioelectronics vol. 20 (2005) 2140–2144, 4/15/.
[27] G. Liu, S.L. Riechers, M.C. Mellen, Y. Lin, Sensitive electrochemical detection of enzymatically generated thiocholine at carbon nanotube modified glassy carbon electrode, Electrochemistry Communications vol. 7 (2005) 1163–1169, 11.
[28] J. Weber, A. Kumar, A. Kumar, S. Bhansali, Novel lactate and pH biosensor for skin and sweat analysis based on single walled carbon nanotubes, Sensors and Actuators B: Chemical vol. 117 (2006) 308–313, 9/12/.
[29] C. Xiang, Y. Zou, L.-X. Sun, F. Xu, Direct electron transfer of cytochrome c and its biosensor based on gold nanoparticles/room temperature ionic liquid/carbon nanotubes composite film, Electrochemistry Communications vol. 10 (2008) 38–41, 1.
[30] S. Carrara, V.V. Shumyantseva, A.I. Archakov, B. Samorì, Screen-printed electrodes based on carbon nanotubes and cytochrome P450scc for highly sensitive cholesterol biosensors, Biosensors and Bioelectronics vol. 24 (2008) 148–150.
[31] D.M.G. Cavallini Andrea, Carrara Sandro, "Comparison of Three Methods of Biocompatible Multi-Walled Carbon Nanotubes Confinement for the Development of Implantable Amperometric ATP Biosensors, Sensor Letters vol. B157 (2011) 216–224.
[32] L. Qian, X. Yang, Composite film of carbon nanotubes and chitosan for preparation of amperometric hydrogen peroxide biosensor, Talanta vol. 68 (2006) 721–727, 1/15/.
[33] I. Taurino, S. Carrara, M. Giorcelli, A. Tagliaferro, G. De Micheli, Comparison of two different carbon nanotube-based surfaces with respect to potassium ferricyanide electrochemistry, Surface Science vol. 606 (2012) 156–160, 2.
[34] T. Momiyama, Electrochemical detection of dopamine from rat dopaminergic neuronal soma using carbon nanotube electrode, Neuroscience Research vol. 68 (Supplement 1) (2010) pe116.
[35] C. Baj-Rossi, G.D. Micheli, S. Carrara, Electrochemical detection of anti-breast-cancer agents in human serum by cytochrome P450-coated carbon nanotubes, Sensors vol. 12 (2012) 6520–6537.
[36] C.E. Banks, T.J. Davies, G.G. Wildgoose, R.G. Compton, Electrocatalysis at graphite and carbon nanotube modified electrodes: edge-plane sites and tube ends are the reactive sites, Chemical Communications (2005) 829–841.
[37] C.E. Banks, R.G. Compton, New electrodes for old: from carbon nanotubes to edge plane pyrolytic graphite, Analyst vol. 131 (2006) 15–21.
[38] A. Holloway, G. Wildgoose, R. Compton, L. Shao, M.H. Green, The influence of edge-plane defects and oxygen-containing surface groups on the voltammetry of acid-treated, annealed and "super-annealed" multiwalled carbon nanotubes, Journal of Solid State Electrochemistry vol. 12 (2008) 1337–1348, 2008/10/01.
[39] C.E. Banks, A. Crossley, C. Salter, S.J. Wilkins, R.G. Compton, Carbon Nanotubes Contain Metal Impurities Which Are Responsible for the "Electrocatalysis" Seen at Some Nanotube-Modified Electrodes, Angewandte Chemie International Edition vol. 45 (2006) 2533–2537.
[40] H.V. Patten, K.E. Meadows, L.A. Hutton, J.G. Iacobini, D. Battistel, K. McKelvey, et al., Electrochemical Mapping Reveals Direct Correlation between Heterogeneous Electron-Transfer Kinetics and Local Density of States in Diamond Electrodes, Angewandte Chemie International Edition vol. 51 (2012) 7002–7006.
[41] I. Dumitrescu, P.R. Unwin, J.V. Macpherson, Electrochemistry at carbon nanotubes: perspective and issues, Chemical Communications (2009) 6886–6901.
[42] I. Streeter, G.G. Wildgoose, L. Shao, R.G. Compton, Cyclic voltammetry on electrode surfaces covered with porous layers: An analysis of electron transfer kinetics at single-walled carbon nanotube modified electrodes, Sensors and Actuators B: Chemical vol. 133 (2008) 462–466, 8/12/.
[43] M. Ammam, J. Fransaer, Glucose/O2 biofuel cell based on enzymes, redox mediators, and Multiple-walled carbon nanotubes deposited by AC-electrophoresis then stabilized by electropolymerized polypyrrole, Biotechnology and Bioengineering vol. 109 (2012) 1601–1609.
[44] S. Carrara, A. Cavallini, V. Erokhin, G. De Micheli, Multi-panel drugs detection in human serum for personalized therapy, Biosensors and Bioelectronics vol. 26 (2011) 3914–3919.
[45] A. D. McNaught and A. Wilkinson, *IUPAC. Compendium of chemical terminology, 2nd ed. (the "Gold Book")* vol. 1669: Blackwell Science Oxford, 1997.
[46] C. Berger, Y. Yi, Z.L. Wang, W.A. de Heer, Multiwalled carbon nanotubes are ballistic conductors at room temperature, Applied Physics A vol. 74 (2002) 363–365, 2002/03/01.
[47] C.C. Moser, J.M. Keske, K. Warncke, R.S. Farid, P.L. Dutton, Nature of biological electron transfer, Nature vol. 355 (1992) 796–802, 02/27/print.
[48] S.N. Daff, S.K. Chapman, R.A. Holt, S. Govindaraj, T.L. Poulos, A.W. Munro, Redox Control of the Catalytic Cycle of Flavocytochrome P-450 BM3†, Biochemistry vol. 36 (1997) 13816–13823, 1997/11/01.
[49] I.V. Kurnikov, D.N. Beratan, Ab initio based effective Hamiltonians for long-range electron transfer: Hartree–Fock analysis, The Journal of chemical physics vol. 105 (1996) p9561.
[50] C.-X. Lei, S.-Q. Hu, G.-L. Shen, R.-Q. Yu, Immobilization of horseradish peroxidase to a nano-Au monolayer modified chitosan-entrapped carbon paste electrode for the detection of hydrogen peroxide, Talanta vol. 59 (2003) 981–988, 4/10/.
[51] I. Taurino, R. Reiss, M. Richter, M. Fairhead, L. Thöny-Meyer, G. De Micheli, et al., Comparative study of three lactate oxidases from Aerococcus viridans for biosensing applications, Electrochimica Acta vol. 93 (2013) 72–79, 3/30/.
[52] X. Ji, R.O. Kadara, J. Krussma, Q. Chen, C.E. Banks, Understanding the Physicoelectrochemical Properties of Carbon Nanotubes: Current State of the Art, Electroanalysis vol. 22 (2010) 7–19.
[53] S. Carrara, Bio/CMOS interfaces and co-design, Springer, 2012.
[54] N. Bistolas, U. Wollenberger, C. Jung, and F. W. Scheller, "Cytochrome P450 biosensors—a review," Biosensors and Bioelectronics, vol. 20, pp. 2408-2423, 6/15/2005.
[55] I. Taurino, A. Magrez, F. Matteini, L. Forró, G. De Micheli, S. Carrara, Direct growth of nanotubes and graphene nanoflowers on electrochemical platinum electrodes, Nanoscale vol. 5 (2013) 12448–12455.
[56] A.F. Holloway, D.A. Craven, L. Xiao, J.D. Campo, G.G. Wildgoose, Developing Random Network Theory for Carbon Nanotube Modified Electrode Voltammetry: Introduction and Application to Estimating the Potential Drop between MWCNT−MWCNT Contacts, The Journal of Physical Chemistry C vol. 112 (2008) 13729–13738, 2008/09/04.
[57] C. Boero, S. Carrara, G. Del Vecchio, L. Calzà, G. De Micheli, Targeting of multiple metabolites in neural cells monitored by using protein-based carbon nanotubes, Sensors and Actuators B: Chemical vol. 157 (2011) 216–224.
[58] A.J. Bard, L.R. Faulkner, Electrochemical methods: fundamentals and applications, vol. 2, Wiley, New York, 1980.
[59] T. Davies, C. Banks, R. Compton, Voltammetry at spatially heterogeneous electrodes, Journal of Solid State Electrochemistry vol. 9 (2005) 797–808, 2005/12/01.
[60] C. Boero, S. Carrara, and G. De Micheli, "Sensitivity enhancement by carbon nanotubes: applications to stem cell cultures monitoring," in Research in Microelectronics and Electronics, 2009. PRIME 2009. Ph. D., 2009, pp. 72-75.
[61] C. Boero, S. Carrara, G. Del Vecchio, L. Calzà, G. De Micheli, Highly sensitive carbon nanotube-based sensing for lactate and glucose monitoring in cell culture," *NanoBioscience*, IEEE Transactions on vol. 10 (2011) 59–67.
[62] I. Heller, J. Kong, H.A. Heering, K.A. Williams, S.G. Lemay, C. Dekker, Individual Single-Walled Carbon Nanotubes as Nanoelectrodes for Electrochemistry, Nano Letters vol. 5 (2004) 137–142, 2005/01/01.
[63] I. Taurino, S. Carrara, M. Giorcelli, A. Tagliaferro, G. De Micheli, Comparing sensitivities of differently oriented multi-walled carbon nanotubes integrated on silicon wafer for electrochemical biosensors, Sensors and Actuators B: Chemical vol. 160 (2011) 327–333.
[64] A. Gasnier, M.L. Pedano, F. Gutierrez, P. Labbé, G.A. Rivas, M.D. Rubianes, Glassy carbon electrodes modified with a dispersion of multi-wall carbon nanotubes in dopamine-functionalized polyethylenimine: Characterization and analytical applications for nicotinamide adenine dinucleotide quantification, Electrochimica Acta vol. 71 (2012) 73–81, 6/1/.
[65] Y.-L. Yao, K.-K. Shiu, Low potential detection of glucose at carbon nanotube modified glassy carbon electrode with electropolymerized poly(toluidine blue O) film, Electrochimica Acta vol. 53 (2007) 278–284, 12/1/.

[66] K.-H. Xue, F.-F. Tao, W. Xu, S.-Y. Yin, J.-M. Liu, Selective determination of dopamine in the presence of ascorbic acid at the carbon atom wire modified electrode, Journal of Electroanalytical Chemistry vol. 578 (2005) 323–329.
[67] S. Shahrokhian, H.R. Zare-Mehrjardi, Application of thionine-nafion supported on multi-walled carbon nanotube for preparation of a modified electrode in simultaneous voltammetric detection of dopamine and ascorbic acid, Electrochimica Acta vol. 52 (2007) 6310–6317, 6/30/.
[68] C. Wang, R. Yuan, Y. Chai, S. Chen, Y. Zhang, F. Hu, et al., Non-covalent iron(III)-porphyrin functionalized multi-walled carbon nanotubes for the simultaneous determination of ascorbic acid, dopamine, uric acid and nitrite, Electrochimica Acta vol. 62 (2012) 109–115, 2/15/.
[69] S. Carrara, V. Bavastrello, D. Ricci, E. Stura, C. Nicolini, Improved nanocomposite materials for biosensor applications investigated by electrochemical impedance spectroscopy, Sensors and Actuators B: Chemical vol. 109 (2005) 221–226.
[70] S. Minnikanti, P. Skeath, N. Peixoto, Electrochemical characterization of multi-walled carbon nanotube coated electrodes for biological applications, Carbon vol. 47 (2009) 884–893.
[71] R.K. Sharma, L. Zhai, Multiwall carbon nanotube supported poly (3, 4-ethylenedioxythiophene)/manganese oxide nano-composite electrode for super-capacitors," Electrochimica Acta vol. 54 (2009) 7148–7155.